MAPS, a turbulence simulator for MCAO

Johann Kolb [*a], Enrico Marchetti [a], Stéphane Tisserand [b], Francis Franza [a], Bernard Delabre [a], Frédéric Gonté [a], Roland Brast [a], Sophie Jacob [b], Fabien Reversat [b]
[a] European Southern Observatory, Karl-Schwarzschild-Str. 2, 85748 Garching, Germany;
[b] SILIOS Technologies, ZI de Peynier Rousset, rue Gaston Imbert prolongée 13790 Peynier, France

ABSTRACT

The Multi-Atmospheric Phase screens and Stars (MAPS) instrument is a powerful tool that has been developed in the framework of the ESO Multi-conjugate Adaptive optics Demonstrator project (MAD). It allows emulating a 3D evolving Paranal-like atmosphere as well as up to 12 sources in a 2 arc minutes field of view, as seen at a Nasmyth focus of one of the VLT. It will be used to perform advanced laboratory tests on MAD before its shipment to Chile.
In this paper we present the opto-mechanical design of MAPS. This one simulates the characteristics of the VLT focus and achieves a high Strehl Ratio over the whole Field of View in the visible as well as in the infrared. A curved entrance plate crowded with fibers emulates various stars configurations including real sky asterisms.
In order to simulate the atmosphere, three rotating Phase Screens are placed in the beam and conjugated with different altitudes. Those are glass plates dig in their surface in a way that the beam passing through is distorted as it would be by an atmospheric turbulent layer. In this poster we also present the process of research that lead to the choice of a reliable technique to imprint the aberrations into the screens, their properties and expected performance.

Key words: Atmospheric turbulence, turbulence generator, phase screens, MCAO, VLT, ion etching

1. INTRODUCTION AND CONCEPT

MAPS has been recognized as a strategic tool for the laboratory testing of the Multi-conjugate Adaptive optics Demonstrator [9, 11, 13, 16]. The goal of MAPS is to emulate a time evolving three-dimensional atmosphere whose induced aberrations are injected into MAD. The characteristics of the atmospheric turbulence shall be similar to those of the Paranal observatory during typical seeing conditions. Different kinds of turbulence simulators have been under investigation for some years [4, 7, 10], but they all have weak points when it is question of full MCAO turbulence emulation. MAPS creates a 2 arcmin FoV beam as seen at the F/15 Nasmyth focus of one of the VLT Units. The strategy is to use an all refractive solution because of its versatility in changing the atmospheric characteristics without increasing the complexity of the system, as for an all reflective or hybrid solution.
The evolving atmosphere is emulated by some rotating transmitting plates, called Phase Screens (PS). The Optical Path Difference (OPD) of the PS substrate is modified locally in order to produce a phase shift in an electromagnetic wave passing through it. The distribution of the phase shift shall follow a typical distribution given by a Von-Kármán spectrum with a finite outer scale. The PSs are positioned along the optical axis in order to emulate the turbulence at different altitudes with the desired spatial and temporal behaviour.
The concept of MAPS is shown in Fig. 1. The Natural Guide Stars (NGS) are emulated by visible-IR light transmitting fibres. Their positions are changeable to create the desired star configuration. A first group of lenses collimates the light beams from the NGSs and allows the telescope pupil to be created. Different PSs are located in the collimated beams to emulate the atmospheric layers at different altitude. One phase screen is located in the telescope pupil to emulate the ground layer. The PSs have different turbulence power according to the expected vertical Cn^2 distribution. The evolving atmosphere is emulated by rotating the PSs at different speeds according to the wind speed vertical profile. The position of the high altitude PS can be slightly varied in order to modify the atmospheric anisoplanetism and the speeds can be adjusted to reproduce a wide range of atmospheric correlation times. Moreover the PSs are interchangeable in order to emulate a selected range of seeing conditions.

* jkolb@eso.org, phone +49.89.32006331; fax +49.89.3202362; http://www.eso.org

A second group of lenses re-images the artificial NGSs whose wavefront quality is degraded by the PSs. The distorted wavefronts are then injected into MAD for MCAO correction and performance evaluation.
Particular care has to be taken when selecting the location of the beam footprints on the different PSs. Because of the rotation, each footprint will experience a differential speed at the edges located along the PS radius. In order to keep this effect as small possible, large PSs have to be considered as well as smaller footprint dimensions. Both conditions are difficult to achieve: large PSs are difficult to manufacture and small footprints require the PSs to be very close to each other, and small pixels size. A reasonable trade-off in the selection of these reduces the differential speed disturbance. The goal achieved is to keep the differential speed smaller than ±50%, which is the average variation of the wind speed inside an 8 meter VLT pupil at Paranal.

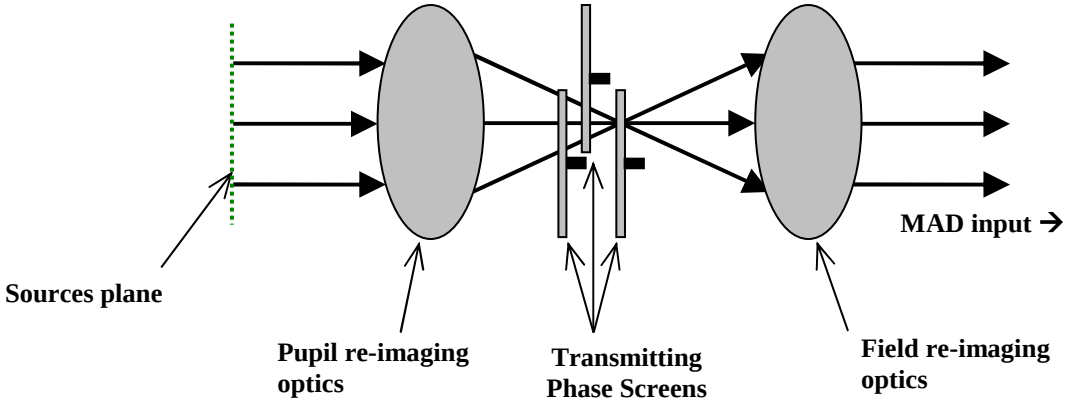

Fig. 1. MAPS concept. The NGS are simulated by optical fibres. A 1:1 imaging system provides to re-image the NGS at the MAD input F/15 focus. The Phase Screens are placed at different altitudes to emulate the turbulent atmospheric layers.

2. OPTICAL DESIGN

The optics of MAPS is constituted of two different groups of lenses (the optical design is shown in Fig. 2):

- The first group provides to collimate the beams from the artificial NGSs placed in a curve field (183 mm radius of curvature), and to create the telescope pupil;
- The second group focuses the disturbed wavefronts of the artificial NGSs on a 2 arcmin focal plane with the VLT F/15 Nasmyth focus characteristics, including the field curvature.

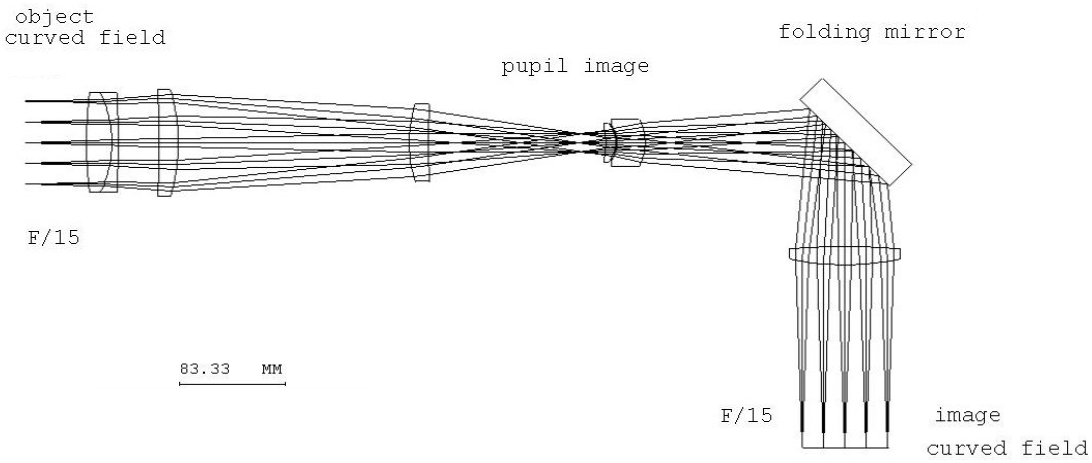

Fig. 2. Optical concept for the MAPS telescope and turbulence simulator. The size of the pupil is 15mm in diameter.

The two groups of optics are manufactured and delivered already mounted in two separate tubes that will then be fixed to the MAPS optical table. As MAPS shall transfer efficiently from 0.5 to 2.5 μm, the choice of the glasses and coatings was done in order to guarantee high transmission up to IR wavelengths.
The purpose of the flat mirror placed in between the second group of lenses is to fold the beam in order to make the turbulence simulator more compact, and to ease its fixation to the MAD bench by reducing the flexure constrains.
The Fig. 3 shows the Strehl Ratio performance of MAPS optics up to 1 arcmin from the FoV centre in the spectral range 0.5-2.5 μm, without PSs. A special care was taken when selecting the optics in order to give preference to an excellent and uniform wavefront quality in the IR range (1 to 2.5 μm) to the prejudice of a good quality in the visible. The Strehl Ration (SR) in this range is still larger than 55% over the whole FoV, whereas the SR in the IR is fairly constant and never worse than 95%.
In the PS space, 1 mm along the optical axis corresponds to ~ 280m in the atmosphere. The two optical blocks have been tested and are well in the specifications.

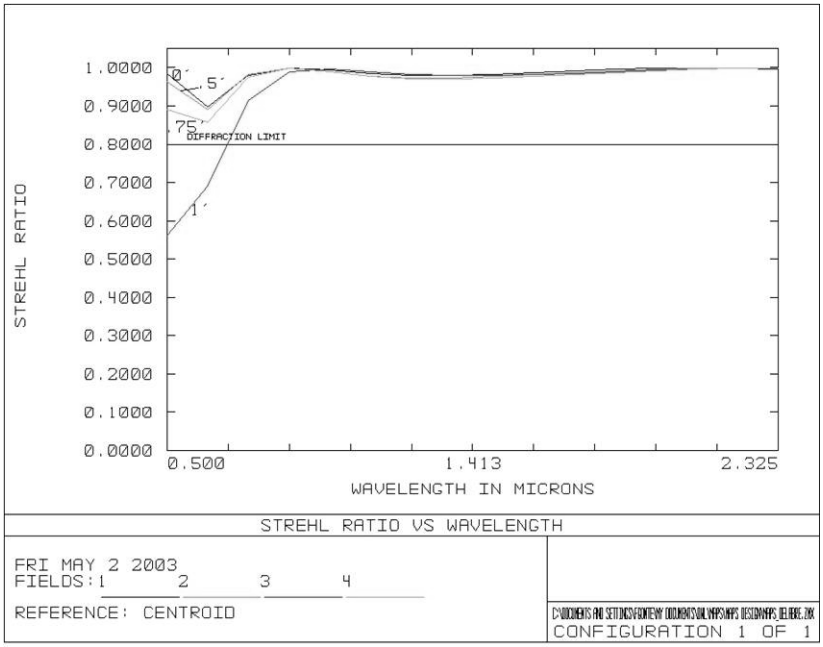

Fig. 3 Strehl Ratio across the FoV of MAPS at different wavelengths (from 500 to 2300 nm).

3. ARTIFICIAL NATURAL GUIDE STARS

MAPS shall simulate up to 12 NGSs for correction and performance evaluation with MAD. The NGS are simulated using single-mode fibres, 9 μm core, transmitting from 0.5 to 2.5 μm. The size of the core is dimensioned to reproduce diffraction limited images of NGSs down to 0.6 μm. The light source is a halogen-tungsten lamp of 150 Watts.
The fibres are distributed in four bunches: one of 12 fibres and three of 8 fibres, so a total of 36 fibres. While the 12 fibres bunch face directly the source, neutral density gelatine filters are placed in front of the 8 fibres bunches in order to dim the light entering. The filters are chosen so that they let respectively 40, 16 and 6.4 % of the light pass through, leading to an attenuation of respectively 1, 2 and 3 magnitudes. Thus MAPS permits to simulate 4 different star magnitudes at the same time (with a maximum of 12 fibres for the brighter magnitude and 8 fibres for the other ones), the magnitude of the brightest star being determined by the dimmer of the source.
The position of the simulated NGS in the field is defined by plugging the fibres on a mask placed in the entrance focal plane of MAPS. The accuracy of positioning of the NGS will be ensured by the use of standard SMA connector for the fibres end, and their female counterpart on the mask. Those connectors are disposed on concentric rings, and each ring is adjusted in depth in order to simulate the telescope field curvature.

The mask is a metallic plate in which are mounted female SMA connectors; the size of those connectors doesn't allow placing two NGS at a closer distance than 18.5 arcsec. The choice of those standards, easy to plug and unplug connectors allows also changing quickly the configuration of the simulated asterism.

In order to simulate NGS asterisms two different solutions are adopted:

- Flexible configuration: a grid of 34 pre-defined star positions has been design for a best coverage of the whole FoV (Fig. 4). This grid will be used to check MAD performances in a first time, and compare them to the results of simulations.
- Real NGS targets: once the target asterisms to be observed on the sky identified [12], special masks will be manufactured according to the desired geometrical configuration, in order to test the system on real star asterism, and to compare later the performance with on-sky measurements.

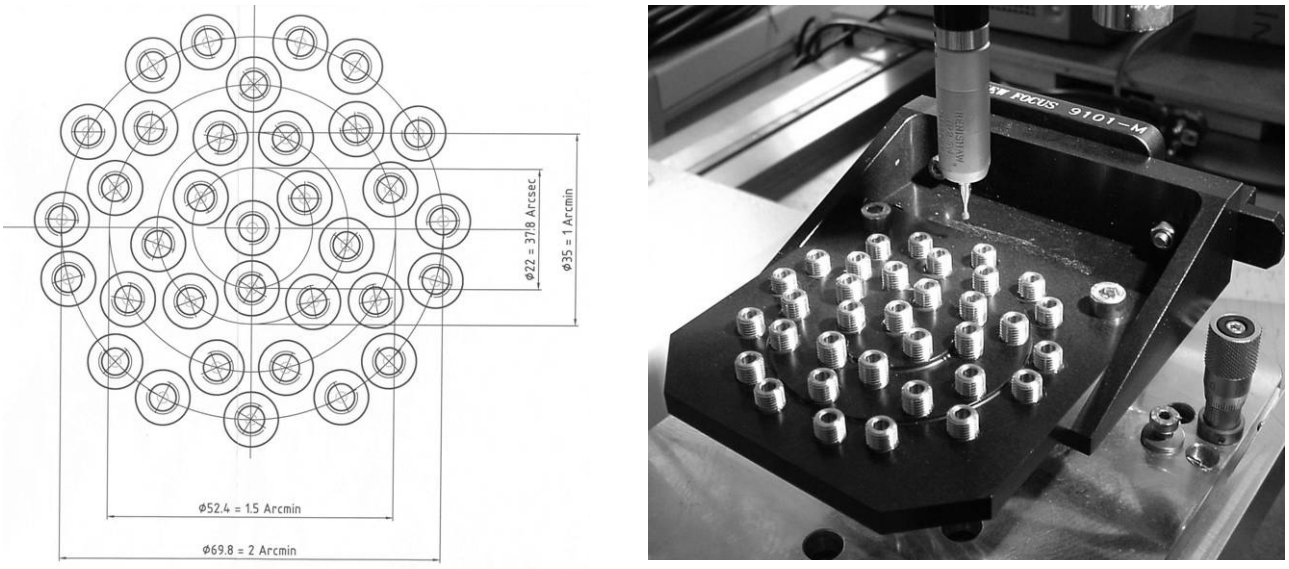

Fig. 4. MAPS entrance plane. Grid of pre-defined positions for plugging the fibers simulating the stars, as designed (left) and during its integration phase (right)

4. PHASE SCREENS

4.1. General Assumptions

MAPS is required to have a set of four phase screens, only 3 of which will be used at any time to simulate two different seeing conditions. The PSs are optical elements capable to transmit the light. They are circular plates (100mm diameter) with a hole at the centre (for fixation of the rotation axis). The PS has encoded on the surface a bi-dimensional aberration with spatial distribution typical of the atmospheric turbulence.
A plane wavefront passing through the PS emerges distorted accordingly to the aberrations encoded on the PS. The aberration is encoded on an annular ring centred on the PS centre, so that the wavefront shift seen through a 15mm pupil centred on the annulus is evolving when the PS is set on rotation. The speed at which ths PS is set in rotation gives the value of the wind speed simulated for this altitude.
The mechanical dimensions of a PS are shown in Fig. 5.

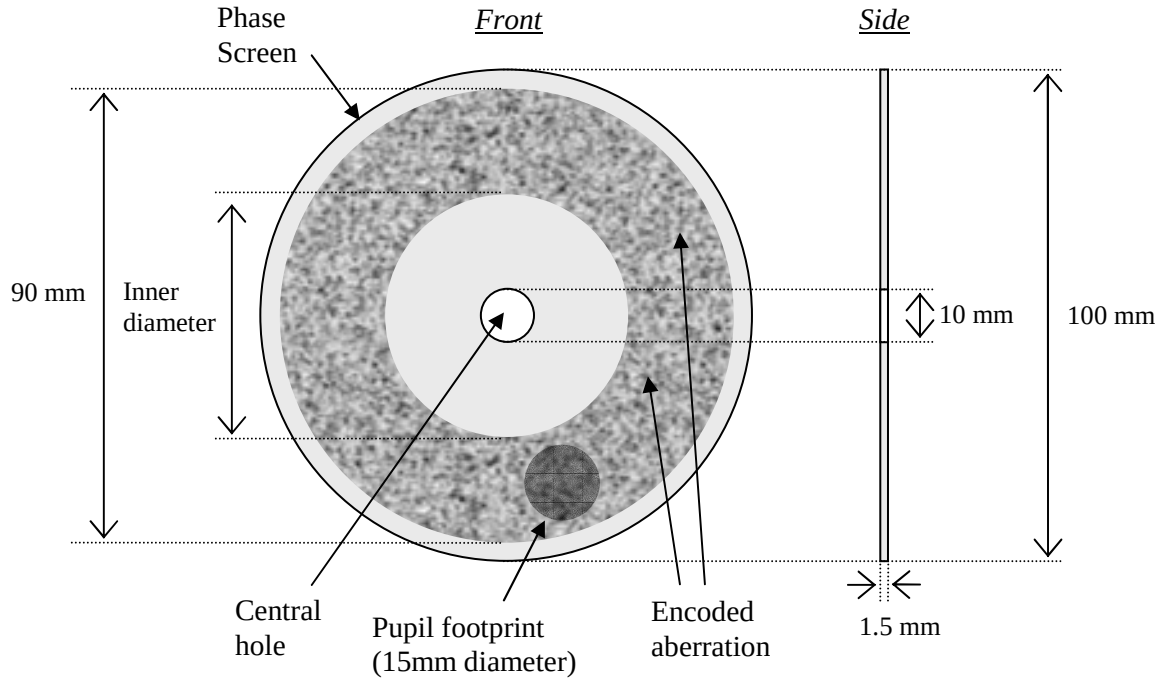

Fig. 5. Dimensions of a Phase Screen. The inner diameter varies depending on the altitude at which the PS is intended to be used.

4.2. Phase maps

The phase screen turbulence data are produced using the invert Fourier transform of a Von Kármán spectrum. Among numerous possible random maps were kept the ones that show the smallest Peak-To-Valley (PTV) phase over their surface, while keeping the global atmospheric properties and particularly the phase variance in the pupil. This property helps for the realization of the PS as a high PTV is always hard to achieve. The size of the phase maps is 900x900 pixels^2, leading to pixels of 100 microns in the case of a ring of aberration of 90mm in diameter.
A finite outer scale of 22 m is considered [14], and the properties of the atmospheric layers we wish to simulate are summarized in the Table 1. PS-01 to PS-04 label four different phase screens, which combination allows reproducing the aberrations induced by the sky of Paranal in two different conditions. The resulting turbulence parameters at the level of the telescope are shown in the Table 2.

	Median @ ZD=30°		
	Altitude	r_0 (0.5μm)	Wind Speed
PS-01	0.0 ± 0.2 km	20 ± 1 cm	7 ± 3 m/s
PS-02	6.0 ± 0.2 km	30 ± 1 cm	13 ± 6 m/s
PS-03	8.5 ± 0.2 km	50 ± 1 cm	30 ± 15 m/s

	Good @ Zenith		
	Altitude	r_0 (0.5μm)	Wind Speed
PS-02	0.0 ± 0.2 km	30 ± 2 cm	7 ± 3 m/s
PS-03	6.0 ± 0.2 km	50 ± 2 cm	13 ± 6 m/s
PS-04	8.5 ± 0.2 km	80 ± 2 cm	30 ± 15 m/s

Table 1. Atmospheric parameters for the MAPS phase screens

Parameter (0.5μm)	Median	Good
r_0 (cm)	14.4 ± 0.6	22.4 ± 1.2
Seeing (“)	0.73 ± 0.03	0.46 ± 0.03
τ_0 (ms)	3.4 ± 0.2	5.5 ± 0.3
θ_0 (arcsec)	2.2 ± 0.1	3.6 ± 0.1

Table 2. Global atmospheric parameters resulting from the use of the Phase Screens defined in the Table 1.

Four phase maps in agreement with those requirements have been found (Fig. 6). Several simulation were performed using those phase maps, such as decomposition on the Zernike polynomials [15], PSF computation, measurement of the variance over one rotation, in order to simulate the aberrations that they will create. Those tests have been carried out for individual PS as well as for theoretical combination of the three PS.
The seeing created by the two different combinations of PSs is given by the FWHM of the integrated PSF at 500 nm wavelength, as shown in Fig. 7. The variance of the projection of the distorted wavefronts on the Zernike polynomials can be compared with the theoretical spectrum given for this r_0 and L_0. We found a good agreement with the two seeings specified, as well as with the spectra.
Simulated PSFs (in the visible and in K band, static and integrated) are shown in Fig. 9. It is interesting to notice the size of the speckles in both cases, much larger in the IR. The residual speckle pattern in the integrated images comes from the fact that the simulations were done at one single wavelength. As foreseen, the size of the integrated IR PSF is smaller that the visible one.

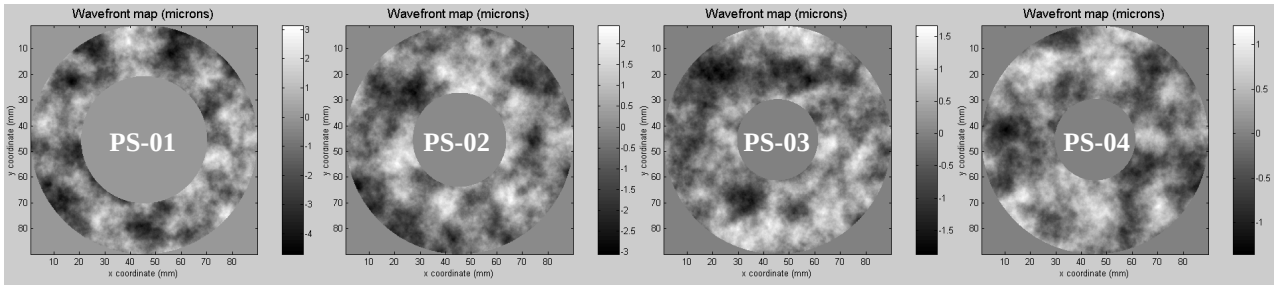

Fig. 6. Phase maps to be imprinted on the 4 phase screens. The width of the imprinted annulus differs, as the footprint of the 2 arcmin meta-pupil increases with the altitude to which the PS is conjugated.

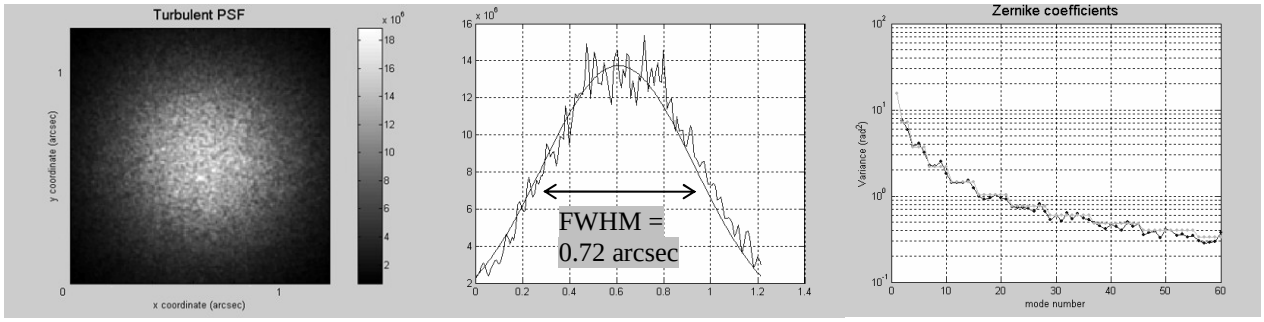

Fig. 7. Simulation result: integrated PSF, PSF profile and variance of the projection on the Zernike polynomials in the case of the combination PS-01/ 02 / 03 (median seeing condition)

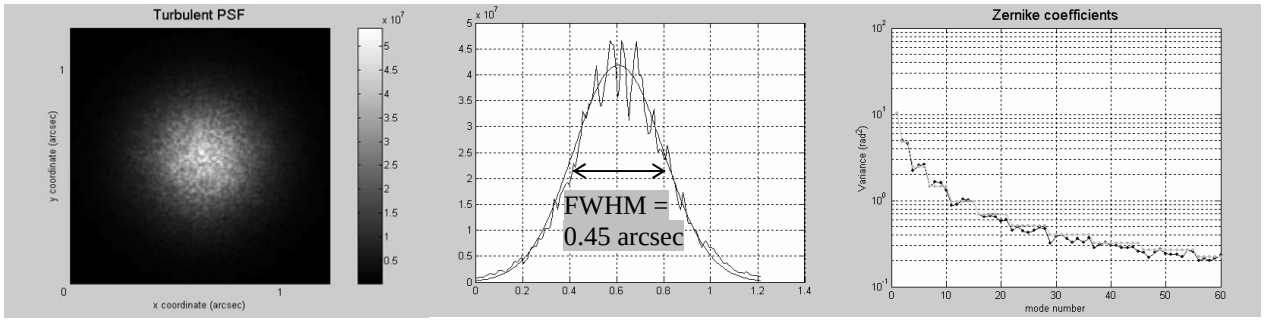

Fig. 8. Simulation result: integrated PSF, PSF profile and variance of the projection on the Zernike polynomials in the case of the combination PS-02/ 03 / 04 (good seeing condition)

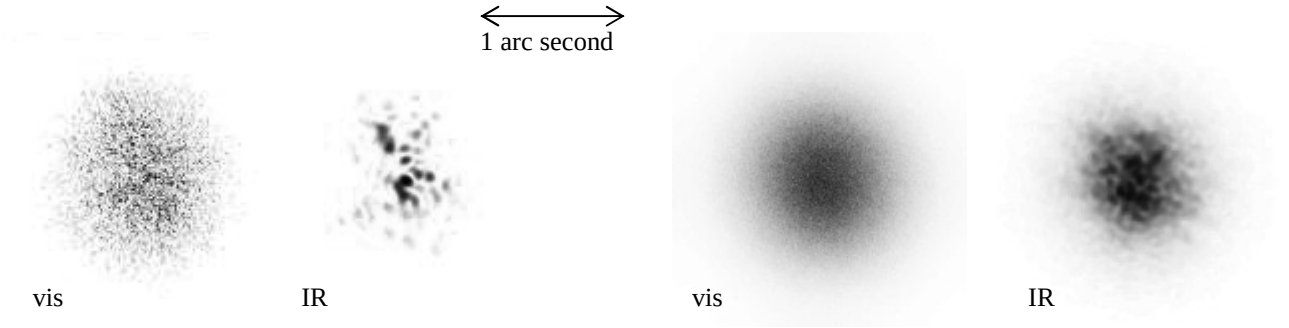

Fig. 9. Simulated visible and IR PSFs, static (left) and integrated over one rotation of the slowest PS (right), resulting from the use of the PS-01, PS-02 and PS-03 in MAPS

4.3. Manufacturing of the phase screens

The methods to produce transmitting PS are numerous [1, 5], and the first method envisaged for the PS of MAPS was an ion-exchange in glass substrate [2, 6]. But after a long process of research and of prototyping, ESO came to an agreement with the company SILIOS Technologies for the manufacturing of several sets of PS satisfying the specifications in terms of mechanical, optical properties and of quality of the aberrations produced. The technique proposed by this company is a wet etching on glass substrate, which description is given below.

SILIOS manufactures the PS in its clean room facilities. 100mm diameter substrates are compatible with off the shelf 4 inches silicon wafer equipments. The basic principle for encoding the 2^N levels of the phase map is to process N individual etching steps which either cumulate or not. The pattern of each individual etching step is defined by a photolithography process (photo-resist deposition, insulation, development). The N patterns are realigned with an accuracy of 0.5 micron (1/200 of a pixel width). The wet etching process is VLSI HF (Very Large Scale Integrated - Hydrogen Fluoride) based. A typical master mask pattern is presented in Fig. 10. 21 master masks were designed (6 for the PS-01, 5 for the PS-02, PS-03 and PS-04). The main issues in the fabrication of the PS are linked to the accuracy of each etching depth and to the uniformity inside the wafer. The technique proposed by SILIOS provides ± 0.7 % as etching depth accuracy (max etching depth is about 20 microns) and ± 0.45 % as uniformity inside the wafer.

A series of tests have been performed on a first realization of the PS-01 and they show a product quality within the specifications.

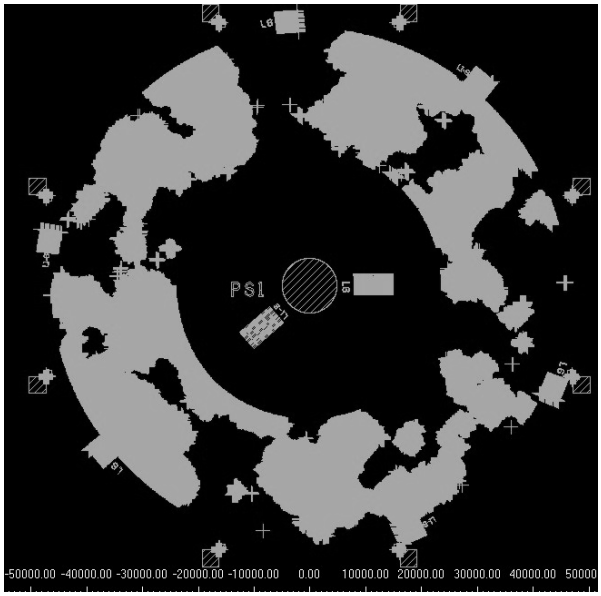

Fig. 10. First mask (out of 6) used to create the PS-01

5. MAPS MECHANICS

MAPS will be located in front of the MAD input and will be used only for laboratory testing. The source for the NGS is located under the bench, far from the MAPS box in order to minimize light contaminations both for MAPS and MAD.
As shown in Fig. 11, the two optical tubes from MAPS are attached to a common plate, itself put at the right height from the bench surface (MAD beam height = 230mm) thanks to some supporting legs standing on the optical table to be screwed on three points to the MAD bench. The fibres support, the optical tube #1 and the whole phase screens system is protected by a removable cover used as a baffle for parasite light Some apertures are opened in this cover to let the cables and fibres pass through, and of course also the beam.
Due to the size of the motors to rotate the PS, it is not possible to place them directly aligned with the axis of the PS, because of conflicts with the optical tube #1 and with the beam. It was then compulsory to put the motors on the sides and to use a system of belts and ball bearings to fit all the components in the available space. Each PS block is thus constituted of the following parts:

- The motor and the reduction gear
- The belt transmitting the rotation to the PS axis
- The axis on which is fixed the PS. It is attached with a system that allows removing easily the PS plate itself and to exchange it with another, in order to switch between the two possible seeing configurations.

The rotations are possible thanks to ball bearings. All the components of a PS block are interdependent, and mounted on the same structure. This structure is movable along the optical axis for the high altitude PS in order to change the isoplanetic angle simulated, and also to facilitate the operation of exchanging the PSs. A system of elongated holes allows stretching the belt.

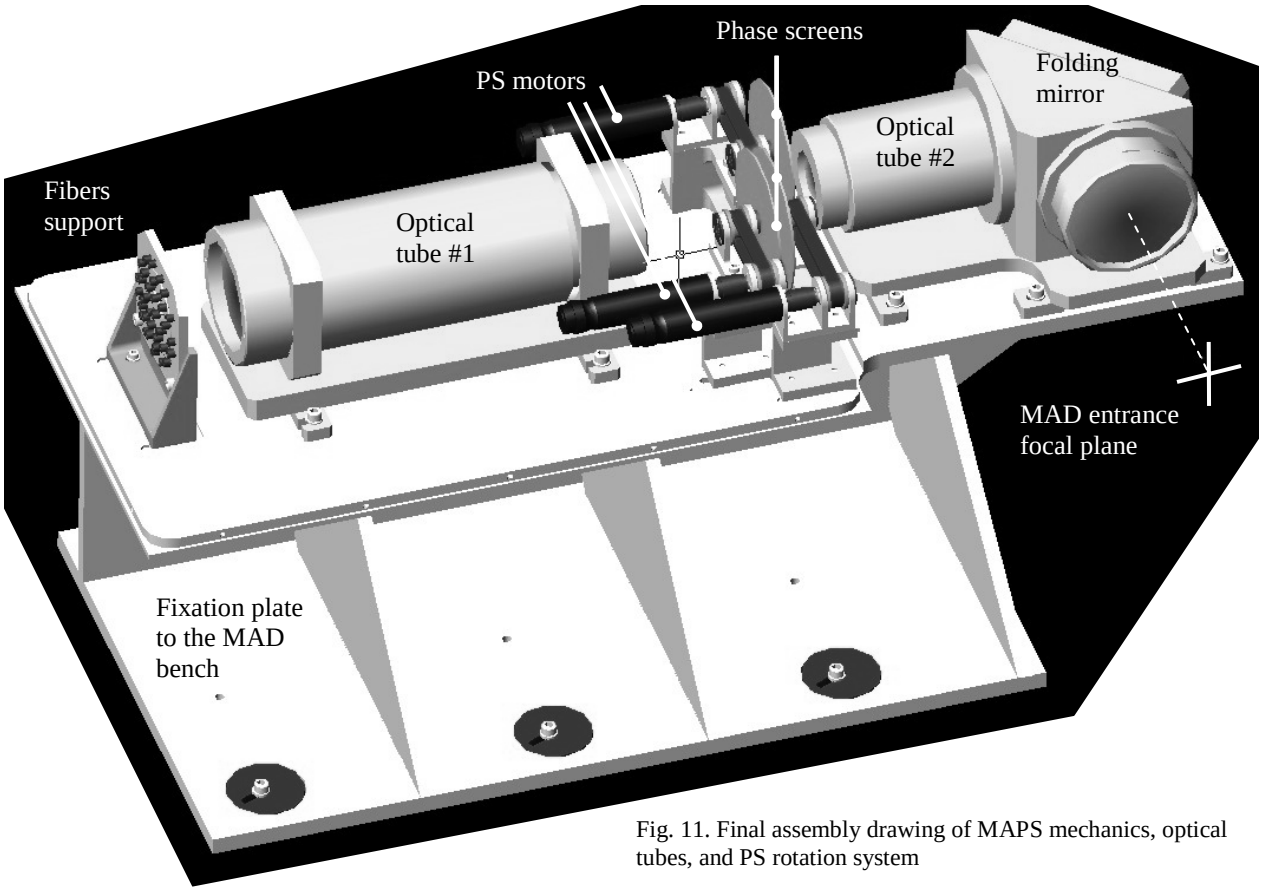

Fig. 11. Final assembly drawing of MAPS mechanics, optical tubes, and PS rotation system

The alignment of the two optical tubes one with respect to the other is done thanks to a guiding tool furnished by the supplier of the optics (Winlight Optics in France). Then the fibers support is placed at the entrance focal plane of the tube #1. The next step consists in finding the pupil position (after placing in the beam some dummy PSs to simulate the additional glass thickness), which is in the output focal plane of the tube #1. The PS rotation blocks being integrated and the PSs mounted in them, they have then to be placed in the beam at the right altitude (a vertical displacement of 200m is acceptable), and well perpendicular to the beam. MAPS is at this point ready to produce turbulence.
When MAPS is placed at the entrance of MAD, their optical axes have to be aligned, as well as the position of the common focus, which corresponds to 5 degrees of freedom in total.

6. MOTORS CONTROL

The three Faulhaber motors rotating the PS are controlled independently by three boards allowing a great accuracy in the speed of the motion. The boards are housed in the MAPS control box, and the control of the speeds is ensured by three potentiometers (Fig. 12 left). The accuracy is again improved by the fact that we use a gear box 1:134 at the output of the motor so that it runs in its linear range although the speed of the PS themselves is quite slow, comprised between 2 and 30 rounds per minute. Also the motors we use are equipped with a feedback sensor of the effective rotation speed of rotation of the axis. Three rigid cables coming out of the back side of the control box (Fig. 12 right) allow placing the control at a distance of up to 1.5 meter from MAPS, and are relayed inside the covered area by more flexible cables connected to the motors.

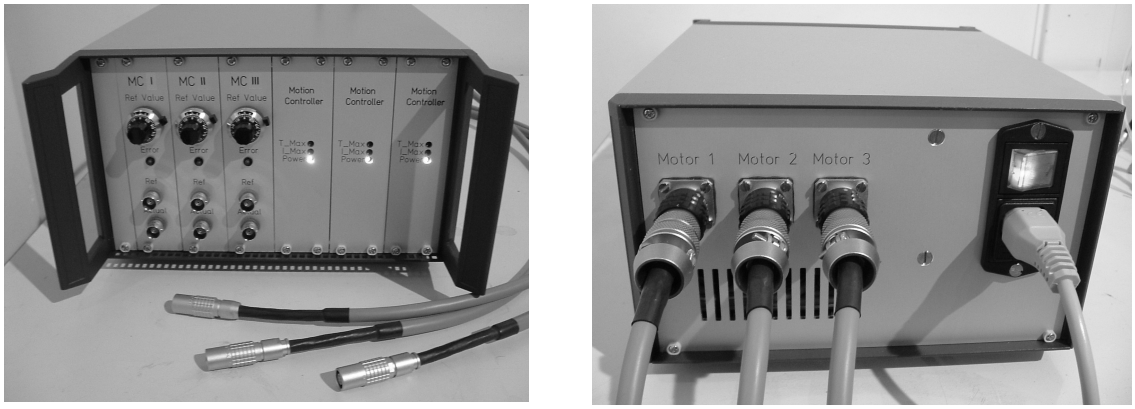

Fig. 12. Front and back side of the PS motors controller box

7. PROJECT STATUS

MAPS is the first full MCAO turbulence simulator ever built, allowing to feed an MCAO instrument as would do a telescope, in terms of wavelength range, FoV and NGS targets. It is compact, easily pluggable to MAD or any other instrument with similar input, as for example ESO's Active Phasing Experiment [8]. The motors and light source controls are totally independent from the instrument. The integration is eased by the fact that the optics blocks are pre-mounted. The turbulence produced is well characterized, reproducible and very similar to the one of the atmosphere, although the number of realizations is limited.
The turbulence simulator is currently integrated and optically aligned in the ESO laboratory (Fig. 13). Only prototype PSs are available for the moment. When the definite ones will be finalized, they will be integrated to the assembly, and the full MAPS system will be tested and the turbulence produced fully characterized.

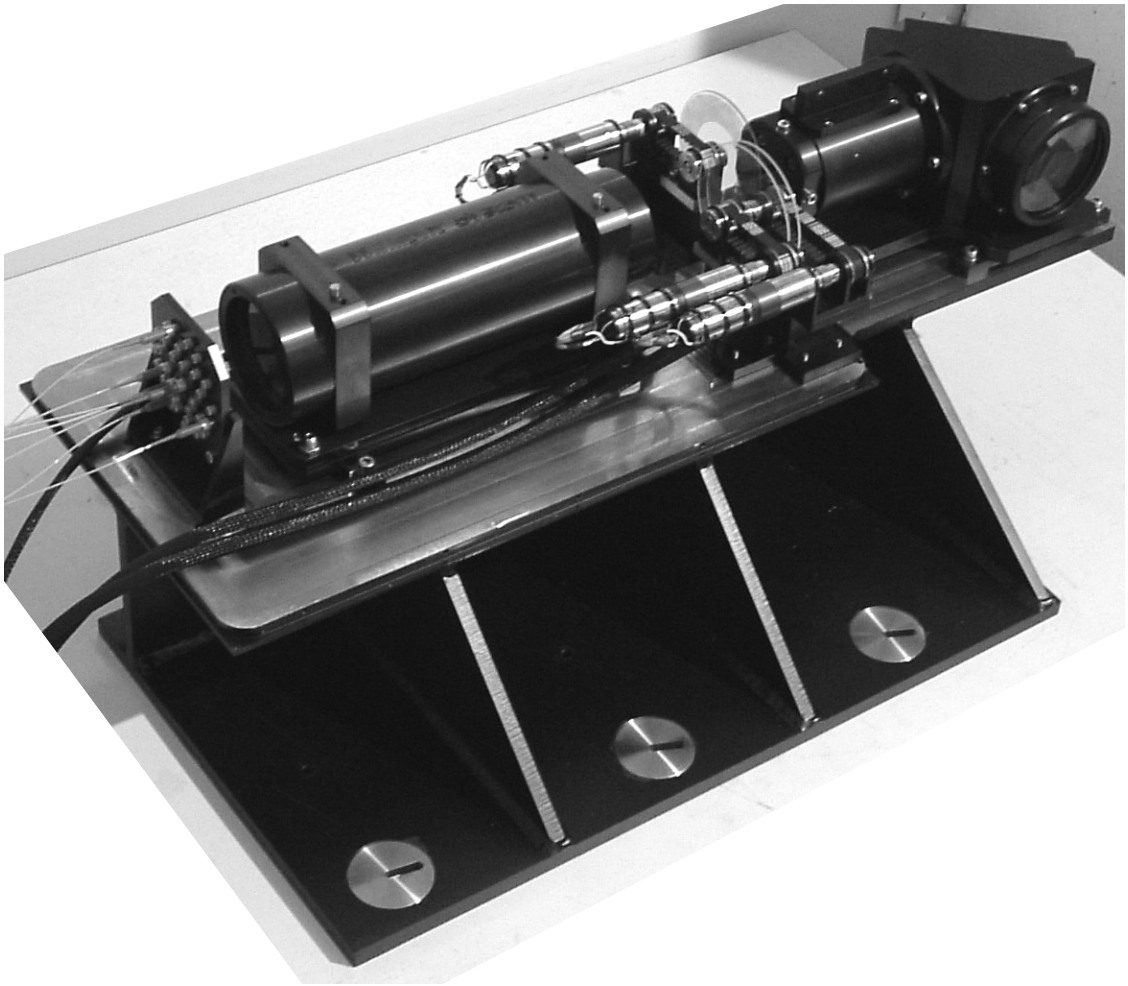

Fig. 13. The turbulence simulator MAPS after its integration and alignment phases

AKNOWLEDGMENT

This work has been partially funded by the European Research and Training Network *Adaptive Optics for Extremely Large Telescopes* with Contract HPRN-CT-2000-00147.

REFERENCES

1. D. J. Butler, S. Hippler, S. Egner, W. Xu, J. Bähr "*Broadband, Static Wave-Front Generation: Na-Ag Ion-Exchange Phase Screens and Telescope Emulation*" Applied Optics, Vol. 43 Issue 14 Page 2813, May 2004
2. D. J. Butler, E. Marchetti, J. Bähr, Wenli Xu, S. Hippler, M. E. Kasper. R. Conan "*Phase screens for astronomical multi-conjugate adaptive optics: application to MAPS*" SPIE 4830, p. 623
3. R. Conan, "*Modélisation des effets de l'échelle externe de cohérence spatiale du front d'onde pour l'observation à Haute Résolution Angulaire en Astronomie*", Ph.D. thesis (Université de Nice-Sophia-Antipolis), 2000

4. C. C. Davis, Y. Zhang, M. L. Plett, P. Polak-Dingels, P. Barbier, D. W. Rush "*Characterization of a liquid-filled turbulence simulator*" in Artificial Turbulence for Imaging and Wave Propagation, Proc. SPIE Vol. 3432, p. 38-49, edited by John D. Gonglewski; Mikhail A. Vorontsov
5. S. M. Ebstein "*Pseudo-random phase plates*" in High-Resolution Wavefront Control: Methods, Devices, and Applications III edited by J. D. Gonglewski, M. A. Vorontsov, M. T. Gruneisen, S. R. Restaino, A. V. Kudryashov, vol. 4493 of Proc. SPIE, article number [4493-24]
6. S. Egner "*Optical turbulence estimation and emulation*" Diploma thesis 2003, University of Heidelberg
7. A. Fuchs, J. Vernin, M. Tallon "*Laboratory simulation of a trubulent layer - Optical and in situ characterization*" Appl. Opt., 35, 1751-1755 (1996)
8. F. Y. J. Gonté, N. Yaitskova, P. Dierickx, A. Courteville, S. Esposito, N. Devaney, K. Dohlen, M. Ferrari, L. Montoya, "*APE: a breadboard to evaluate new phasing technologies for a future European giant optical telescope*" Advancements in Adaptive Optics, SPIE Proceedings, 5489, article number [5489-144], 2004
9. N. Hubin, E. Marchetti, E. Fedrigo, R. Conan, R. Ragazzoni, E. Diolaiti, M. Tordi, G. Rousset, T. Fusco, P. Y. Madec, D. Butler, S. Hippler, S. Esposito "*The ESO MCAO demonstrator MAD: a European collaboration*", Proc. of the ESO Conference on 'Beyond Conventional Optics', May 7-10, Venice, 2001
10. G.D. Love, P. Clark, C.N. Dunlop, T.-.Kelly, M.Langlois, R. Myers and R. Sharples '*Emulating Multiconjugate Turbulence*", Proc. of the ESO Conference on 'Beyond Conventional Optics', May 7-10, Venice, 2001
11. E. Marchetti, R. Brast, B. Delabre, R. Donaldson, E. Fedrigo, F. Franza, N. Hubin, J. Kolb, M. Le Louarn, J. Lizon, S. Oberti, R. Reiss, J. Santos, R. Ragazzoni, C. Arcidiacono, A. Baruffolo, E. Diolaiti, J. Farinato, E. Vernet-Viard, "*MAD status report*", Advancements in Adaptive Optics, SPIE Proceedings, 5490, article number [5490-17], 2004
12. E. Marchetti, R. Falomo, D. Bello, N. Hubin "*A search for star asterisms for natural guide star based MCAO correction in Beyond Conventional Adaptive Optics*". Eds. Ragazzoni R., Hubin N. and Esposito S. 1.82 + AFOSC
13. E. Marchetti, N. Hubin, E. Fedrigo, J. Brynnel, B. Delabre, R. Donaldson, F. Franza, R. Conan, M. Le Louarn, C. Cavadore, A. Balestra, D. Baade, J. Lizon, R. Gilmozzi, G. J. Monnet, R. Ragazzoni, C. Arcidiacono, A. Baruffolo, E. Diolaiti, J. Farinato, E. Vernet-Viard, D. J. Butler, S. Hippler, and A. Amorin, "*MAD the ESO multi-conjugate adaptive optics demonstrator*" in Adaptive Optical System Technologies II. Edited by Wizinowich, Peter L.; Bonaccini, Domenico, vol. 4839 of Proc. SPIE, pp. 317-328, Feb. 2003.
14. F. Martin, R. Conan, A. Tokovinin, A. Ziad, H. Trinquet, J. Borgnino, A. Agabi, M. Sarazin "*Optical parameters relevant for High Angular Resolution at Paranal from GSM instrument and surface layer contribution*", Astron. Astrophys. Suppl. Ser. 144, 39-44, May 2000
15. R. J. Noll "*Zernike polynomials and atmospheric turbulence*" JOSA, 66:207 (1976)
16. http://www.eso.org/projects/aot/mad/